Asian Journal of Andrology (2023) 25, 331–338
www.asiaandro.com; www.ajandrology.com

Open Access

ORIGINAL ARTICLE

Male Health

The protective effects and underlying mechanisms of dapagliflozin on diabetes-induced testicular dysfunction

Zhi-Chao Luo[1,*], Zi-Run Jin[1,*], Ya-Fei Jiang[2], Tian-Jiao Wei[2], Ya-Lei Cao[1], Zhe Zhang[1,3], Rui Wei[2], Hui Jiang[1,3]

Male diabetic individuals present a marked impairment in fertility; however, knowledge regarding the pathogenic mechanisms and therapeutic strategies is unsatisfactory. The new hypoglycemic drug dapagliflozin has shown certain benefits, such as decreasing the risk of cardiovascular and renal events in patients with diabetes. Even so, until now, the effects and underlying mechanisms of dapagliflozin on diabetic male infertility have awaited clarification. Here, we found that dapagliflozin lowered blood glucose levels, alleviated seminiferous tubule destruction, and increased sperm concentrations and motility in leptin receptor-deficient diabetic *db/db* mice. Moreover, the glucagon-like peptide-1 receptor (GLP-1R) antagonist exendin (9–39) had no effect on glucose levels but reversed the protective effects of dapagliflozin on testicular structure and sperm quality in *db/db* mice. We also found that dapagliflozin inhibited the testicular apoptotic process by upregulating the expression of the antiapoptotic protein B-cell lymphoma 2 (BCL2) and X-linked inhibitor of apoptosis protein (XIAP) and inhibiting oxidative stress by enhancing the antioxidant status, including total antioxidant capacity, total superoxide dismutase (SOD) activity, and glutathione peroxidase (GPx) activity, as well as decreasing the level of 4-hydroxynonenal (4-HNE). Exendin (9–39) administration partially reversed these effects. Furthermore, dapagliflozin upregulated the glucagon-like peptide-1 (GLP-1) level in plasma and GLP-1R expression by promoting AKT8 virus oncogene cellular homolog (Akt) phosphorylation in testicular tissue. Exendin (9–39) partially inhibited Akt phosphorylation. These results suggest that dapagliflozin protects against diabetes-induced spermatogenic dysfunction via activation of the GLP-1R/phosphatidylinositol 3-kinase (PI3K)/Akt signaling pathway. Our results indicate the potential effects of dapagliflozin against diabetes-induced spermatogenic dysfunction.

Asian Journal of Andrology (2023) **25**, 331–338; doi: 10.4103/aja202242; published online: 15 July 2022

Keywords: dapagliflozin; diabetes; glucagon-like peptide-1 receptor; male infertility; oxidative stress

INTRODUCTION

It is estimated that nearly 10% of couples suffer from infertility worldwide, and almost half of these cases are primarily caused by male factors.[1] Male reproductive health problems, especially infertility, impose serious challenges due to substantial psychological and social distress, as well as a considerable economic burden on families suffering from infertility.[2] The pathogenesis of male infertility mainly includes disorders of spermatogenesis and sperm maturation, presenting clinically as oligozoospermia, asthenozoospermia, teratozoospermia, and azoospermia, *etc*.[3] Many factors, including congenital, environmental, and metabolic factors, could lead to oligoasthenozoospermia, but due to its complicated etiological mechanism and the extraordinary heterogeneity of its clinical presentation in patients, effective and targeted therapeutic interventions remain unclear.[2,4]

The prevalence of diabetes has continued to grow globally, with an overall estimated prevalence of 10.5% (536.6 million people) among the 20- to 79-year-old population in 2021, which leads to the consensus that diabetes has become a critical public health problem worldwide.[5] Moreover, studies in patients and animal models have revealed that diabetes has detrimental influences on the male reproductive system, as this disease may impair male fertility in terms of testicular histopathology, sperm quality, and DNA damage.[6,7] Hypoglycemic drugs such as insulin and metformin have been verified to be capable of improving or restoring male fertility in diabetic animal models.[8,9] On the other hand, some antidiabetic drugs might exert adverse effects on male fertility.[10,11] Sodium-glucose co-transporter-2 (SGLT2) inhibitors represent a newly developed, effective, and safe strategy for diabetes treatment that has been shown to exert multiple metabolic benefits, such as improving the effectiveness of blood glycemic control and high-density lipoprotein cholesterol regulation. These compounds also have weight-reducing and antihypertensive effects.[12–14] Recently, SGLT2 inhibitors, including dapagliflozin and canagliflozin, have been described as being capable of reducing the risk of developing cardiovascular events and diabetic renal diseases.[15–17] This gives clues that SGLT2 inhibitors are able to protect the diabetes-targeted

[1]Department of Urology, Peking University Third Hospital, Beijing 100191, China; [2]Department of Endocrinology and Metabolism, Peking University Third Hospital, Beijing 100191, China; [3]Department of Reproductive Medicine Center, Peking University Third Hospital, Beijing 100191, China.
[*]These authors contributed equally to this work.
Correspondence: Dr. H Jiang (jianghui55@163.com) or Dr. R Wei (weirui@bjmu.edu.cn)
Received: 26 February 2022; Accepted: 23 May 2022

cardiovascular system and kidney. We therefore inferred that these inhibitors may positively affect male fertility and spermatogenesis since testicular damage also develops in diabetes-induced hyperglycemia impairment.[7] The level of glucagon-like peptide-1 (GLP-1), a peptide secreted from the distal small intestine that exerts blood glucose-regulating effects, was upregulated in the plasma and pancreatic cells of dapagliflozin-treated diabetic mice.[13] Furthermore, exendin (9–39), a unique competitive antagonist of the GLP-1 receptor (GLP-1R), inhibited the hypoglycemic effect of insulin stimulated by GLP-1.[18,19] However, whether dapagliflozin can affect diabetes-induced male infertility through the activation of GLP-1R remains unexplored. Therefore, it is necessary and important to explore the exact effects of dapagliflozin on male fertility caused by diabetes.

In the present study, first, the influences of dapagliflozin on spermatogenesis and sperm quality in diabetic mice were investigated; and second, the underlying mechanisms were explored.

MATERIALS AND METHODS

Animals and interventions

All animal experiments in our study were validated by the Peking University Animal Care and Use Committee (Peking University, Beijing, China; No. LA2021371). Male BKS.Cg-Dock7^{m}+/+Lepr^{db}/Nju mice (*db/db*, 8 weeks old; Nanjing Biomedical Research Institution of Nanjing University, Nanjing, China) were group-housed following conventional methods with free access to food and water and maintained at 23.0°C ± 3.0°C on a 12 h/12 h light/dark cycle. The diabetic condition of the mice (after 1 week of adaptation) was verified if the fasting blood glucose was ≥11.1 mmol l^{-1} or random blood glucose was ≥16.7 mmol l^{-1}. The diabetic mice were randomly divided into three groups with 9 mice undergoing vehicle treatment (deionized water [ddH_2O]; labeled *db/db*), 10 mice receiving dapagliflozin (labeled Dapa), and 6 mice administered dapagliflozin + exendin (9–39) (a GLP-1R antagonist; labeled Ex) for 5 weeks. Mice were intragastrically administered 1 mg kg^{-1} dapagliflozin (a gift from AstraZeneca Pharmaceutical Co., Ltd., London, UK) or an equal amount of vehicle (ddH_2O) once per day according to a previous study.[13] Mice in the Ex group were treated with 25 nmol kg^{-1} per day of exendin (9–39) (cat# E7269, Sigma–Aldrich, St. Louis, MO, USA) using an ALZET® osmotic pump (Alzet model 1007D, Durect, Cupertino, CA, USA). We used 9 littermate *db/m* mice of the same age as the normal control group.

Body weight, blood glucose, and hormone measurements

We measured the random body weights of the mice from 8:00 am to 9:30 am and the fasting body weight after 15 h of fasting. Blood samples were collected from the tail vein, and the blood glucose levels were measured using an OneTouch Ultra glucometer (LifeScan, Milpitas, CA, USA) following the glucose oxidase method. The value was recorded as 33.3 mmol l^{-1} if the blood glucose level was higher than 33.3 mmol l^{-1} (upper testing limit of the glucometer). For hormone detection, a mixture of aprotinin (1 μg ml^{-1}; cat# A1250000, Sigma–Aldrich), heparin sodium (1000 IU ml^{-1}; cat# H3149, Sigma–Aldrich), and dipeptidyl peptidase-4 inhibitor (50 μmol l^{-1}; cat# DPP4-010, Millipore, Billerica, MA, USA) was added to each blood sample. Blood samples were evaluated with specific enzyme-linked immunosorbent assay (ELISA) kits for detecting active GLP-1 (cat# RAB0201-1KT, Sigma–Aldrich). Seven, 9, 10, and 6 mice in the *db/m*, *db/db*, Dapa, and Ex groups were used for ELISA experiments, respectively.

Hematoxylin and eosin (H&E) staining

Under deep anesthesia, the mouse testes were removed and fixed in 10% neutral buffered formalin for no more than 24 h. After dehydration through an ethanol series, the fixed testes were embedded in paraffin and sectioned on slides. Paraffin sections (5 μm thick) were then stained with H&E (cat# BA4097 and cat# BA4098, BaSO, Zhuhai, China) as previously described.[20] Histological analysis was performed using a light microscope (Leica DM 4000, Leica Biosystems, Nussloch, Germany). The area of the normal seminiferous tubules was measured by Image-Pro Plus software (version 6.0, Media Cybernetics, Rockville, MD, USA). One testicle from 4 mice in each group was used to conduct H&E staining and measure the area of the normal seminiferous tubules.

Sperm count and motility assessment

Mature sperm in the mouse cauda epididymis were prepared as described before.[21] Two caudal epididymis samples were placed into human tubal fluid (HTF) medium (cat# MR-070, Sigma–Aldrich). Then, we slightly cut the cauda of the epididymis into three pieces for incubation at 37°C for 5 min. We performed sperm concentration and motility analyses using the computer-assisted semen analysis system (CASA; WLJY-9000, Beijing Weili Co., Ltd., Beijing, China) according to the laboratory manual of the World Health Organization.[3] Parameters including sperm concentration (×10^{6} ml^{-1}), rapid progressive motility (grade A; in %), progressive motility (grade A + B; in %), curve-line velocity (VCL; in μm s^{-1}), straight-line velocity (VSL; in μm s^{-1}), linearity (LIN; in %), average path velocity (VAP; in μm s^{-1}), amplitude of lateral head displacement (ALH; in μm), and straightness (STR; in %) were evaluated. At least 200 sperm were counted for each assay. Seven, 8, 7, and 6 mice in the *db/m*, *db/db*, Dapa, and Ex groups were used for semen analysis, respectively.

Terminal deoxynucleotidyl transferase-mediated dUTP nick-end labeling (TUNEL) assay and apoptotic index assessment

Testes fixed in 4% paraformaldehyde were cryoprotected in 20% sucrose in phosphate-buffered saline (PBS) at 4°C for a few days. The tissue was then cut on a cryostat (10 μm thick) and thaw-mounted on gelatin-coated slides for the TUNEL assay. Apoptotic cells in the testicular tissue were identified with a One Step TUNEL Apoptosis Assay Kit (cat# C1088, Beyotime, Shanghai, China). Testicular sections were simultaneously stained with the nuclear counterstaining marker 4',6-diamidino-2-phenylindole (DAPI; cat# C1002, Beyotime) for 10 min at room temperature and then observed under a confocal microscope (Zeiss LSM710, Carl Zeiss Microscopy GmbH, Jena, Germany) at excitation wavelengths of 488 nm (green) and 405 nm (blue). The number of apoptotic seminiferous tubules and cells was counted. Cells with green-stained nuclei were considered to be TUNEL-positive, and five areas of each slide were randomly selected for cell counting. The apoptotic index was calculated as follows: apoptotic index = TUNEL-positive cells count/total cells count × 100%.[22] One testicle from 4 mice in each group was used to conduct the TUNEL assay.

Western blotting

A section of mouse testicular tissue was immediately homogenized in ice-cold lysis buffer (cat# P0013B, Beyotime). To extract the total protein in the supernatant, the homogenized samples were centrifuged (Centrifuge 5425 R, Eppendorf, Hamburg, Germany) at 12 000*g* and 4°C for 10 min. Then, the protein concentration was measured with a bicinchoninic acid (BCA) assay kit (cat# 23227, Thermo Scientific, Waltham, MA, USA). According to the methods described before, the protein expression was assessed by Western blotting.[21] Protein samples (40 μg) were denatured and then separated by sodium dodecyl sulfate–polyacrylamide gel electrophoresis (SDS–PAGE) using a 10%

separating gel and transferred to a polyvinylidene fluoride membrane (Bio-Rad, Hercules, CA, USA). Then, we blocked the membranes with 5% bovine serum albumin or nonfat milk in Tris-buffered saline Tween (TBST) for 1 h at room temperature followed by incubation of the membranes at 4°C overnight with the following primary antibodies: rabbit monoclonal anti-BCL2 (1:1000; cat# 3498, Cell Signaling Technology, Boston, MA, USA), rabbit monoclonal anti-BAX (1:1000; cat# 14796, Cell Signaling Technology), rabbit polyclonal anti-XIAP (1:1000; cat# 2042, Cell Signaling Technology), rabbit monoclonal anti-Caspase3 (1:1000; cat# 9662, Cell Signaling Technology), rabbit monoclonal anti-Caspase8 (1:1000; cat# 4790, Cell Signaling Technology), mouse monoclonal anti-Caspase9 (1:1000; cat# 9508, Cell Signaling Technology), rabbit polyclonal anti-4-hydroxynonenal (4-HNE; 1:1000; cat# ab46545, Abcam, Cambridge, UK), goat polyclonal anti-GLP-1R (1:1000; cat# TA326758, OriGene, Wuxi, China), rabbit polyclonal anti-AKT8 virus oncogene cellular homolog (Akt; 1:1000; cat# 9272, Cell Signaling Technology), rabbit polyclonal anti-phospho-Akt (Thr308) (pAkt; 1:1000; cat# 9275, Cell Signaling Technology), and mouse monoclonal anti-α-tubulin (1:2000; cat# 3873, Cell Signaling Technology). We washed the blots in TBST for incubation with horseradish peroxidase (HRP)-conjugated secondary antibodies, including goat anti-mouse IgG-HRP (1:2000; cat# sc-2005, Santa Cruz, Dallas, TX, USA), goat anti-rabbit IgG-HRP (1:2000; cat# sc-2004, Santa Cruz), and rabbit anti-goat IgG-HRP (1:2000; cat# sc-2768, Santa Cruz). Using an enhanced chemiluminescence detection kit (cat# 32106, Thermo Scientific), the protein bands were visualized with Tanon 5200 autoradiography equipment (Tanon, Shanghai, China). The bands were quantified with ImageJ imaging analysis software (National Institutes of Health, Bethesda, MD, USA). One testicle from 4 or 5 mice per group was used for Western blotting to detect the protein expression and 4-HNE levels.

Total antioxidant capacity (T-AOC), superoxide dismutase (SOD) activity, glutathione peroxidase (GPx) activity, hydrogen peroxide, and malondialdehyde (MDA) level measurements

A piece of testicular tissue from each mouse in each of the four groups was immediately homogenized in ice-cold PBS. Total protein extraction and protein concentration measurements were performed as described above to analyze the enzyme activities. The T-AOC of testicular tissue was measured by the rapid 3-ethylbenzthiazoline-6-sulfonic acid method (cat# S0121, Beyotime). Total SOD activity and GPx activity in testicular tissue were measured with a total superoxide dismutase assay kit (cat# S0109, Beyotime) with nitroblue tetrazolium (NBT) and a glutathione peroxidase assay kit (cat# S0056, Beyotime) with nicotinamide adenine dinucleotide phosphate (NADPH), respectively. The levels of hydrogen peroxide and MDA in testicular tissue were detected using a hydrogen peroxide detection kit (cat# S0038, Beyotime) and an MDA detection kit (cat# S0131, Beyotime) based on the chromogenic reaction between MDA and thiobarbituric acid (TBA).[23–26] The T-AOC, SOD, GPx, hydrogen peroxide, and MDA levels were normalized to that of the total protein. Five or six mice from each group were used in these experiments to measure the level of oxidative stress in testicular tissue.

Statistical analyses

We used GraphPad Prism version 8.0 (GraphPad Software, La Jolla, CA, USA) to perform statistical analyses and normality tests. All immunofluorescence staining and quantitative biochemical data were representative of at least three experimental replicates. We used the two-tailed unpaired Student's *t* test or one-way analysis of variance (ANOVA) with Sidak's *post hoc* test for comparison of two groups or multiple comparisons. We expressed all data as the mean ± standard error of mean (s.e.m.), and we considered differences of $P < 0.05$ to be statistically significant. The normality test table of all data was provided as **Supplementary Table 1**.

RESULTS

Dapagliflozin lowers blood glucose in db/db mice independent of GLP-1R pathways

The fasting and random body weights of *db/db* mice were significantly higher than those of *db/m* mice at baseline and after 5 weeks of treatment with vehicle (both $P < 0.001$; **Supplementary Figure 1a** and **1b**). Five weeks of dapagliflozin treatment had no effect on the body weights of *db/db* mice (**Supplementary Figure 1a** and **1b**). The fasting and random blood glucose levels were significantly increased in *db/db* mice compared with *db/m* mice ($P < 0.01$ and $P < 0.001$, respectively). Dapagliflozin significantly decreased the blood glucose levels compared with the *db/db* mice, especially the fasting blood glucose level ($P < 0.01$ and $P < 0.001$, respectively; **Supplementary Figure 1c** and **1d**).

In a previous study, we proved that the level of active GLP-1 in plasma could be upregulated by dapagliflozin.[13] It is therefore interesting to determine whether GLP-1R and its signaling pathways contribute to the protective effects of dapagliflozin. We used exendin (9–39) to block the GLP-1R pathways, as it can completely antagonize the glucagonostatic effect of GLP-1.[27] Our results demonstrated that exendin (9–39) treatment did not influence the body weights or blood glucose levels of dapagliflozin-treated *db/db* mice (**Supplementary Figure 1a**–**1d**). These results revealed that dapagliflozin could lower the blood glucose levels of *db/db* mice and the hypoglycemic effect did not depend on GLP-1R.

Dapagliflozin alleviates the destruction of seminiferous tubules in db/db mice

We then conducted H&E staining on the mouse testicular tissue to determine whether dapagliflozin could affect the fertility of *db/db* mice. H&E staining suggested that in vehicle-treated *db/db* mice, the spermatogenic cells and spermatids in the seminiferous tubules were prominently decreased and almost all of the seminiferous tubules were disordered compared with *db/m* mice (**Figure 1a**–**1d**). Treatment with dapagliflozin partly alleviated the destruction of the seminiferous tubules in *db/db* mice, but the ameliorative influences of dapagliflozin were partially reversed by exendin (9–39) (**Figure 1c**–**1h**). The area of normal seminiferous tubules in *db/db* mice was significantly decreased when compared with *db/m* mice ($P < 0.001$; **Figure 1i**). Dapagliflozin treatment partly alleviated this outcome in *db/db* mice, while these ameliorative effects were partially reversed by exendin (9–39) (both $P < 0.001$; **Figure 1i**).

Dapagliflozin restores the decreases in sperm concentration and motility in db/db mice

As treatment with dapagliflozin could partly alleviate the destruction of the seminiferous tubules in *db/db* mice, we were inspired to further determine whether treatment with dapagliflozin could improve the concentration and motility of *db/db* mouse sperm. The CASA results revealed that sperm concentration and rapid progressive and progressive sperm motility were significantly reduced in vehicle-treated *db/db* mice compared with *db/m* mice (all $P < 0.001$; **Figure 2a**–**2c**). Other sperm motility parameters, including VSL, VCL, VAP, LIN, and ALH, were also significantly decreased in vehicle-treated *db/db* mice ($P < 0.001$, $P < 0.001$, $P < 0.001$, $P < 0.05$,

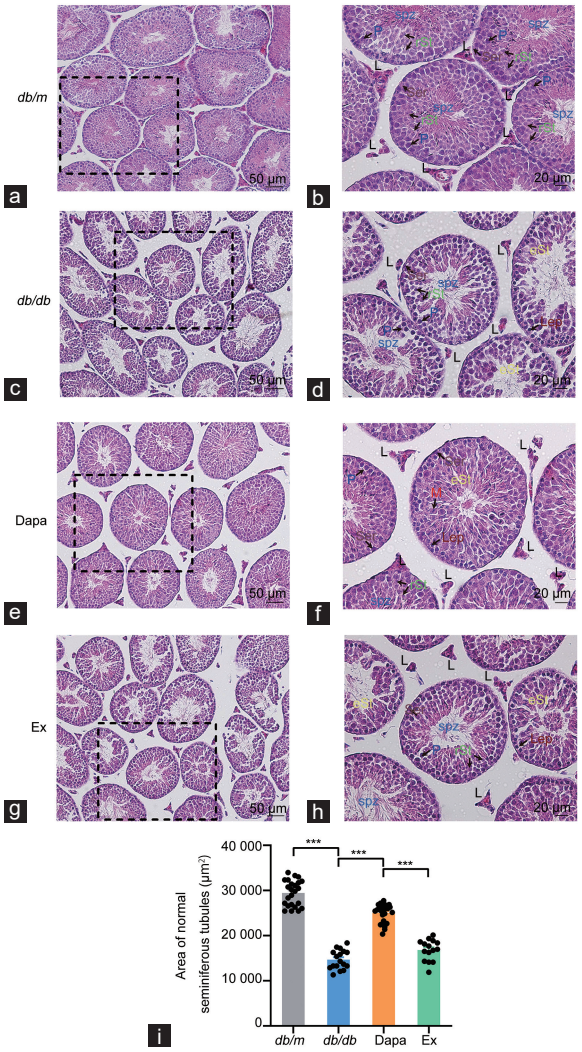

Figure 1: H&E staining of the testicular tissue of *db/m* mice and *db/db* mice treated with dapagliflozin (Dapa) and dapagliflozin + exendin (9–39) (Ex). H&E staining of the testicular tissue of *db/m* mice with (**a**) scale bar = 50 μm and (**b**) scale bar = 20 μm. H&E staining of the testicular tissue of *db/db* mice with (**c**) scale bar = 50 μm and (**d**) scale bar = 20 μm. H&E staining of the testicular tissue of Dapa mice with (**e**) scale bar = 50 μm and (**f**) scale bar = 20 μm. H&E staining of the testicular tissue of Ex mice with (**g**) scale bar = 50 μm and (**h**) scale bar = 20 μm. Arrows with abbreviations in different colors indicate different types of cells. (**i**) Area of normal seminiferous tubules. $n = 4$ mice per group. All data are presented as the mean ± standard error of mean. $^{***}P < 0.001$. H&E: hematoxylin and eosin; P: pachytene spermatocytes; rSt: round spermatids; eSt: elongating spermatids; Lep: leptotene spermatocytes; M: meiotic spermatocytes; L: Leydig cells; Ser: Sertoli cells.

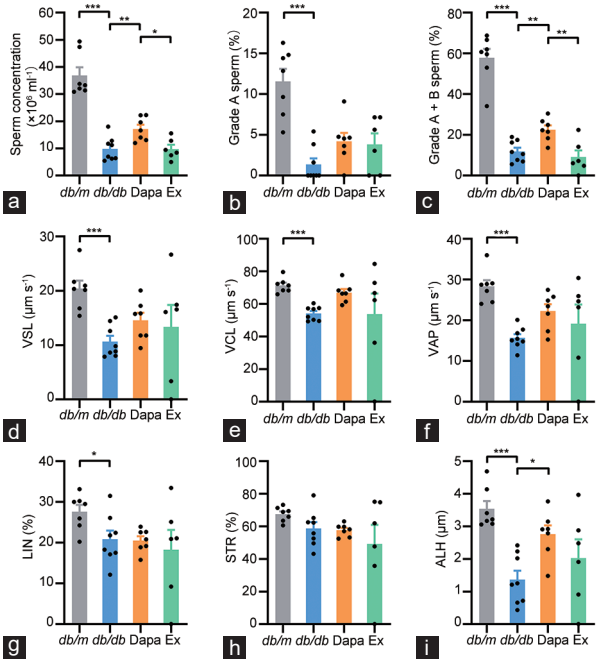

Figure 2: The concentrations and motility of the sperm from *db/m* mice and *db/db* mice treated with dapagliflozin (Dapa) and dapagliflozin + exendin (9–39) (Ex). (**a**) Sperm concentrations. (**b**) Rapid progressive motility (grade A sperm) of the sperm. (**c**) Progressive motility (grade A + B sperm) of the sperm. (**d**) VSL of the sperm. (**e**) VCL of the sperm. (**f**) VAP of the sperm. (**g**) LIN of the sperm. (**h**) STR of the sperm. (**i**) ALH of the sperm. $n = 7$, 8, 7, and 6 mice for *db/m*, *db/db*, Dapa, and Ex groups, respectively. All data are presented as the mean ± standard error of mean. $^{*}P < 0.05$, $^{**}P < 0.01$, $^{***}P < 0.001$. VSL: straight-line velocity; VCL: curve-line velocity; VAP: average path velocity; LIN: linearity; STR: straightness; ALH: amplitude lateral head displacement.

and $P < 0.001$, respectively; **Figure 2d–2g** and **2i**). STR was not altered among all four groups (**Figure 2h**). Treatment with dapagliflozin partly recovered the reductions in sperm concentration, progressive motility, and ALH in *db/db* mice ($P < 0.01$, $P < 0.01$, and $P < 0.05$, respectively; **Figure 2a, 2c,** and **2i**). However, the protective effects of dapagliflozin were partially abrogated by exendin (9–39) treatment ($P < 0.05$ and $P < 0.01$, respectively; **Figure 2a** and **2c**).

Dapagliflozin downregulates testicular tissue apoptosis in db/db mice

The fact that dapagliflozin could ameliorate the disordered seminiferous tubule morphology and increase the sperm concentration in *db/db* mice urged us to investigate the apoptotic status in testicular tissue. First, the TUNEL assay results showed that the number of TUNEL-positive seminiferous tubules and cells in the testicular tissue significantly increased in *db/db* mice ($P < 0.01$ and $P < 0.001$, respectively) but significantly decreased in dapagliflozin-treated *db/db* mice ($P < 0.01$ and $P < 0.001$, respectively), while exendin (9–39) partially reversed the antiapoptotic effects of dapagliflozin in *db/db* mice ($P < 0.01$ and $P < 0.05$, respectively; **Figure 3**). Then, we further investigated the protein expression of antiapoptotic proteins (BCL2 and XIAP) and proapoptotic proteins (BAX, Caspase3, Caspase8, and Caspase9) in the testicular tissue of the four groups of mice. The Western blotting results showed that dapagliflozin treatment significantly upregulated the decreased BCL2 protein expression in *db/db* mice, whereas exendin (9–39) partly reversed the improvement mediated by dapagliflozin, but the protein expression of BAX was not altered among the four groups ($P < 0.01$, $P < 0.001$, and $P < 0.01$, respectively; **Figure 4a–4c**). Moreover, the decreased protein expression of XIAP in *db/db* mice was ameliorated by dapagliflozin treatment and exendin (9–39) partly reversed this effect (all $P < 0.05$); moreover, dapagliflozin treatment had no effect on the protein expression of Caspase3, Caspase8, and Caspase9, although the last two proteins were significantly upregulated in the *db/db* group (both $P < 0.05$; **Figure 4d–4h**). These results suggested that dapagliflozin could improve spermatogenic function in the testicular tissue of *db/db* mice mainly by regulating the expression of antiapoptotic proteins, and the protective effects were partly dependent on GLP-1R.

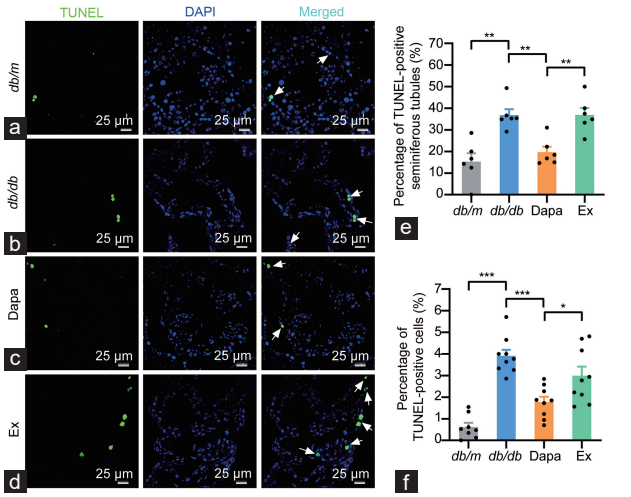

Figure 3: TUNEL assay of the testicular tissue from *db/m* mice and *db/db* mice treated with dapagliflozin (Dapa) and dapagliflozin + exendin (9–39) (Ex). Representative images of the TUNEL-positive seminiferous tubules and the TUNEL-positive cells in testicular tissue of (**a**) *db/m* mice, (**b**) *db/db* mice, (**c**) Dapa mice, and (**d**) Ex mice. Scale bars = 25 μm. White arrows indicated the TUNEL-positive cells in testicular tissue. (**e**) Quantitative analysis of the TUNEL-positive seminiferous tubules and (**f**) the TUNEL-positive cells. $n = 4$ mice per group. All data are presented as the mean ± standard error of mean. $^{*}P < 0.05$, $^{**}P < 0.01$, $^{***}P < 0.001$. TUNEL: terminal deoxynucleotidyl transferase-mediated dUTP nick-end labeling; DAPI: 4',6-diamidino-2-phenylindole.

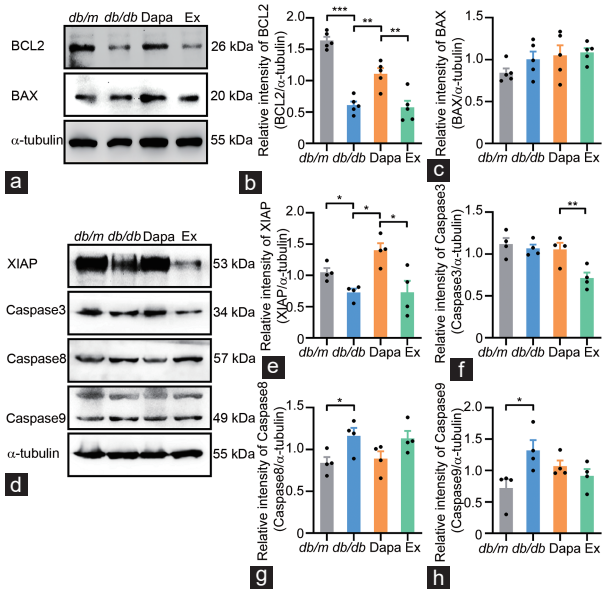

Figure 4: Apoptosis-associated protein expression in the testicular tissue from *db/m* mice and *db/db* mice treated with dapagliflozin (Dapa) and dapagliflozin + exendin (9–39) (Ex). (**a**) Representative plots of the expression of the antiapoptotic protein BCL2, the proapoptotic protein BAX and the protein α-tubulin. Quantitative analysis of the expression of (**b**) the antiapoptotic protein BCL2 and (**c**) the proapoptotic protein BAX. (**d**) Representative plots of the expression of the antiapoptotic protein XIAP, the proapoptotic proteins Caspase3, Caspase8 and Caspase9, and the protein α-tubulin. Quantitative analysis of the expression of (**e**) the antiapoptotic protein XIAP, (**f**) the proapoptotic protein Caspase3, (**g**) the proapoptotic protein Caspase8, and (**h**) the proapoptotic protein Caspase9. $n = 5$ mice per group in **a**–**c**, $n = 4$ mice per group in **d**–**h**. All data are presented as the mean ± standard error of mean. $^{*}P < 0.05$, $^{**}P < 0.01$, $^{***}P < 0.001$. BCL2: B-cell lymphoma 2; BAX: BCL2-associated X protein; XIAP: X-linked inhibitor of apoptosis protein.

Dapagliflozin decreases oxidative stress in the testicular tissue of db/db mice

Previous studies have indicated that GLP-1 can downregulate oxidative phosphorylation and reduce oxidative stress.[28,29] Hence, we investigated the alteration in testicular tissue oxidative stress status in dapagliflozin-treated *db/db* mice. Compared with *db/m* mice, the T-AOC and total SOD activity and GPx activity decreased in the testicular tissue of *db/db* mice (all $P < 0.05$) but increased in that of the dapagliflozin-treated *db/db* mice (all $P < 0.05$; **Figure 5a**–**5c**). The levels of hydrogen peroxide and MDA showed no difference among all four groups (**Figure 5d** and **5e**). The level of 4-HNE, a biomarker of oxidative stress, was upregulated in vehicle-treated *db/db* mice ($P < 0.05$) but downregulated in the testicular tissue of dapagliflozin-treated mice ($P < 0.05$; **Figure 5f**). Exendin (9–39) treatment partially reversed the decreased level of 4-HNE resulting from dapagliflozin treatment ($P < 0.05$; **Figure 5f**). These results suggested that dapagliflozin could decrease oxidative stress in the testicular tissue of *db/db* mice, and the protective effects depend partly on the GLP-1R signaling pathway.

Dapagliflozin activates the GLP-1R/phosphatidylinositol 3-kinase (PI3K)/Akt signaling pathway in the testicular tissue of db/db mice

A previous study showed that the activation of GLP-1R involved phosphorylation of protein kinase A (PKA), cAMP response element-binding protein (CREB), and Akt, which can regulate the expression of antiapoptotic proteins, including BCL2 and XIAP, as well as proapoptotic proteins, including BAX and the caspase family.[30] To further determine whether GLP-1/GLP-1R signaling pathways were involved in the protective effects of dapagliflozin on testicular tissue, we detected alterations in the plasma GLP-1 levels as well as the protein expression of GLP-1R and its downstream signaling pathways in mouse testicular tissue. Data from the present study revealed that the GLP-1 level in plasma and GLP-1R protein expression in testicular tissue were significantly downregulated in the vehicle-treated *db/db* mice ($P < 0.001$ and $P < 0.01$, respectively) but significantly upregulated in dapagliflozin-treated *db/db* mice ($P < 0.001$ and $P < 0.05$, respectively; **Figure 6a** and **6b**). Additionally, the plasma GLP-1 level increased, and GLP-1R protein expression decreased in testicular tissue after exendin (9–39) treatment (both $P < 0.001$; **Figure 6a** and **6b**). The ratio of pAkt/Akt significantly decreased in vehicle-treated *db/db* mouse testicular tissue, whereas Akt phosphorylation was improved by treatment with dapagliflozin and partially reversed by exendin (9–39) ($P < 0.05$, $P < 0.01$, and $P < 0.01$, respectively; **Figure 6c**). These results indicated that dapagliflozin activated the GLP-1R/PI3K/Akt signaling pathway in the testicular tissue of *db/db* mice.

DISCUSSION

In the present study, we found that dapagliflozin, an SGLT2 inhibitor, could reduce blood levels, relieve diabetes-induced impairment of sperm concentration and motility, and exert its antiapoptotic effects in testicular tissue by upregulating the expression of antiapoptotic proteins. Furthermore, dapagliflozin decreased oxidative stress by increasing the T-AOC in the testicular tissue of *db/db* mice. Moreover, the plasma GLP-1 and GLP-1R levels and Akt phosphorylation in the *db/db* group of mice were increased after treatment with dapagliflozin. The GLP-1R antagonist exendin (9–39) partially reversed the reproductive improvements mediated by dapagliflozin, suggesting that the protective effects of dapagliflozin on male fecundity might be associated with the activation of GLP-1R and its downstream PI3K/Akt signaling pathway.

Diabetes can impair male reproduction by damaging the testicular structure, inducing spermatogenic dysfunction and apoptosis, impairing

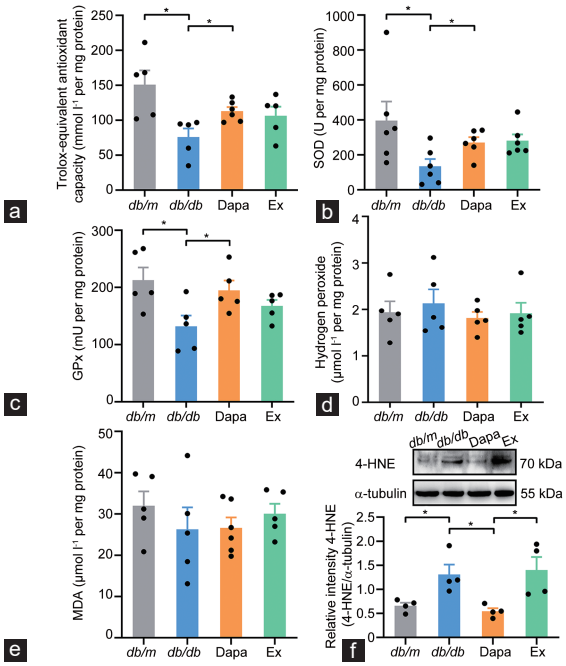

Figure 5: Alterations in the oxidative stress status in the testicular tissue of *db/m* mice and *db/db* mice treated with dapagliflozin (Dapa) and dapagliflozin + exendin (9–39) (Ex). (**a**) Total antioxidant capacity represented by trolox-equivalent antioxidant capacity, $n = 5$ or 6 mice per group. Level of (**b**) total SOD activity ($n = 6$ mice per group), (**c**) GPx activity ($n = 5$ mice per group), (**d**) hydrogen peroxide ($n = 5$ mice per group), (**e**) MDA ($n = 5$ or 6 mice per group), and (**f**) 4-HNE ($n = 4$ mice per group). All data are presented as the mean ± standard error of mean. $^{*}P < 0.05$. SOD: superoxide dismutase; GPx: glutathione peroxidase; MDA: malondialdehyde; 4-HNE: 4-hydroxynonenal.

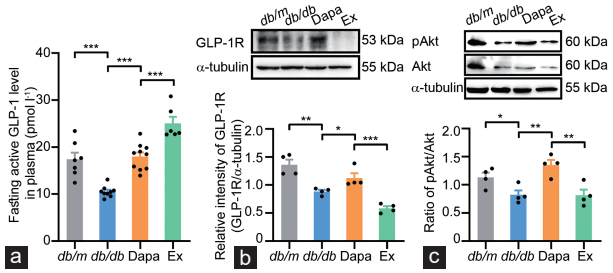

Figure 6: Alterations in the levels of fasting active GLP-1 in plasma, GLP-1R and the downstream signaling pathway components in the testicular tissue of *db/m* mice and *db/db* mice treated with dapagliflozin (Dapa) and dapagliflozin + exendin (9–39) (Ex). (**a**) GLP-1 levels in plasma. (**b**) Protein expression of GLP-1R detected by Western blotting and quantitative analysis of GLP-1R. (**c**) Protein expression of pAkt and Akt detected by Western blotting and quantitative analysis of the ratio of pAkt/Akt. $n = 7$, 9, 10, and 6 mice in the *db/m*, *db/db*, Dapa, and Ex groups for GLP-1 levels in plasma, respectively; and $n = 4$ mice per group for Western blotting. All data are presented as the mean ± standard error of mean. $^{*}P < 0.05$, $^{**}P < 0.01$, $^{***}P < 0.001$. Akt: AKT8 virus oncogene cellular homolog; pAkt: phospholation-Akt; GLP-1: glucagon-like peptide-1; GLP-1R: glucagon-like peptide-1 receptor.

sperm quality, dysregulating the hypothalamic–pituitary–gonad (HPG) axis, and disordering hormone secretion.[7] Our results from H&E staining and TUNEL assays showed that diabetes induced male reproductive damage, as the seminiferous tubules in the testicular tissue of *db/db* mice were generally disordered, and the spermatogenic cells and spermatids in the seminiferous tubules were prominently decreased, which might be due in part to apoptosis. We also found that the sperm concentration and sperm motility in *db/db* diabetic mice were decreased. The prolonged hyperglycemia that occurs with diabetes can generate and accumulate advanced glycation end products (AGEs) by activating oxidative stress and increasing reactive oxygen species (ROS) in the testis, epididymis, and sperm of diabetic patients.[31,32] The excessive production of ROS can induce autophagy and further aggravate testicular oxidative damage under diabetic conditions.[33] In accordance with these findings, the present study revealed that the T-AOC, total SOD activity, and GPx activity decreased, while the level of 4-HNE increased in the testicular tissue of *db/db* mice. Therefore, the diabetes-induced impairment of male fertility could be partly explained by the increasing levels of apoptosis and oxidative stress.

Good diabetes management is the key to minimizing diabetic complications. Some antidiabetic drugs, such as insulin, metformin, and *Momordica charantia* extract, have been proven to have protective effects on male reproductive activity. These drugs can restore HPG axis function by normalizing the levels of luteinizing hormone and testosterone, improving the histopathological changes in the testes, decreasing spermatogenic and Sertoli cell apoptosis, rescuing the impaired sperm motility, and reducing sperm genomic instability caused by DNA fragmentation in diabetic animal models.[8,34–36] However, some antidiabetic drugs have been reported to have adverse effects on sperm quality. For example, glibenclamide reduces sperm viability in ejaculated human semen samples due to its ability to block K_{ATP} channels and induce Ca^{2+} influx.[10] Therefore, it is of great value to investigate whether antidiabetic drugs can truly improve diabetes-related male reproductive dysfunction. SGLT2 inhibitors, including empagliflozin, canagliflozin, and dapagliflozin, represent a new type of oral antidiabetic medicines that inhibit glucose reabsorption in the kidney.[37] Whether SGLT2 inhibitors provide some benefit to male reproductive function remains unclear, and the underlying mechanism has not yet been revealed. In this study, we found that dapagliflozin alleviated testicular destruction and restored sperm quality in *db/db* mice. In addition, our results revealed that dapagliflozin inhibited apoptosis and oxidative stress by increasing the expression of antiapoptotic proteins and the T-AOC, total SOD activity, and GPx activity.

Notably, most of the protective effects produced by antidiabetic drugs on male reproductive function rely on their glucose-lowering effects. For instance, metformin and sulfonylureas might improve male reproductive function in individuals with type 2 diabetes; however, these compounds might cause undesirable or even detrimental effects on the reproductive system when used in individuals without diabetes or those with conditions other than type 2 diabetes.[38] Surprisingly, in our study, treatment with exendin (9–39) did not alter the hypoglycemic effect but partly reversed the reproductive protection conferred by dapagliflozin. Dapagliflozin attenuates diabetes-induced cardiovascular events and renal failure independent of the glucose-lowering effect.[39,40] Our previous study showed that dapagliflozin exerted protective effects on pancreatic beta cells by heightening their proliferation and differentiation.[13] Together, these results indicate that the reproductive protection shown by dapagliflozin might be partly dependent on its hypoglycemic effect, which is probably due to other potential mechanisms, such as direct activation of the GLP-1R/PI3K/Akt signaling pathway.

Our study, together with others, has reported that SGLT2 inhibitors, including dapagliflozin, upregulate the circulating GLP-1 level in diabetic rodents and humans.[13,41–43] GLP-1 exerts its protective effects mainly through GLP-1R. Previous study has reported that

exendin (9–39) can upregulate plasma GLP-1 levels through the disruption of a negative feedback loop with neighboring somatostatin-secreting enteroendocrine cells.[44] Together with the results of this study, we think that exendin (9–39) may exert its effects through a similar mechanism. GLP-1R is expressed in the testis, primarily located in the middle section of human sperm as well as Sertoli cells in mouse and human testes. GLP-1 or GLP-1R agonists can improve sperm motility and reduce proinflammatory cytokine expression, mitochondrial membrane potential, and oxidative damage.[45–47] Therefore, we wanted to determine whether the protective effects of dapagliflozin depend on GLP-1R and its downstream signaling pathways. In this study, we demonstrated that dapagliflozin could upregulate plasma GLP-1 levels and increase GLP-1R expression and Akt phosphorylation. Most importantly, exendin (9–39) treatment reversed the protective effects of dapagliflozin on diabetic mouse testis, including the improvements in sperm concentration and motility and the antiapoptotic and antioxidative stress effects. Exendin (9–39) did not affect the VSL, VCL, VAP, LIN, STR, or ALH of dapagliflozin-treated *db/db* mice, which might be partly because dapagliflozin treatment had no significant effect on the aforementioned parameters in *db/db* mice. Altogether, these results suggested that the improvements induced by dapagliflozin on diabetic male testicular dysfunction may be partly mediated by the GLP-1R/PI3K/AKT signaling pathway. Previous studies have shown that GLP-1 and its analogs, such as liraglutide, can upregulate GLP-1R expression in many kinds of tissue, including renal tissue and cartilage.[48,49] However, further study is needed to uncover the underlying mechanism of how GLP-1 upregulates GLP-1R protein expression, but we speculated that the protective effects of dapagliflozin on diabetic testicular dysfunction might be due to its direct effects on GLP-1R.

There are several limitations to this study. First, further investigation is needed regarding which kind of testicular cells dapagliflozin exerts its protective effects on, even though we know that dapagliflozin can protect against diabetes-induced testicular dysfunction by upregulating the GLP-1 level in plasma and GLP-1R protein expression and increasing the level of Akt phosphorylation in the testicular tissue of *db/db* mice. Second, it is intriguing that exendin (9–39) treatment can augment the increased GLP-1 level in the plasma of dapagliflozin-treated diabetic mice. Further verification is needed to determine whether there is also a negative feedback loop involving the neighboring somatostatin-secreting enteroendocrine cells, which is similar to other studies. Finally, whether dapagliflozin exerts its protective effects on male patients with diabetes-induced infertility needs further clinical investigation.

CONCLUSIONS

Treatment with dapagliflozin alleviates impaired spermatogenesis, improves sperm quality, and ameliorates apoptosis and the overall oxidative stress status in the testicular tissue of diabetic mice. These effects probably occur via the activation of the GLP-1R/PI3K/Akt signaling pathway. Dapagliflozin may be a promising treatment for male patients with both diabetes and impaired fertility.

AUTHOR CONTRIBUTIONS

RW and HJ designed the study, and reviewed and revised the manuscript. ZCL, ZRJ, YFJ, and TJW developed the animal models. ZCL, ZRJ, and YLC performed the experimental research. ZCL, ZRJ, and ZZ performed the statistical analysis and made the diagrams. ZCL and ZRJ drafted the manuscript. All authors read and approved the final manuscript.

COMPETING INTERESTS

All authors declared no competing interests.

ACKNOWLEDGMENTS

We are grateful for the sacrifice of the experimental animals and the technical support of the technicians in Reproductive Medicine Center of Peking University Third Hospital, Beijing, China. This work was supported by the National Natural Science Foundation of China (81901535 and 82071698), the Natural Science Foundation of Beijing Municipality (7222208), and the National Key Research & Developmental Program of China (2021YFC2700203).

Supplementary Information is linked to the online version of the paper on the *Asian Journal of Andrology* website.

REFERENCES

1 Vander Borght M, Wyns C. Fertility and infertility: definition and epidemiology. *Clin Biochem* 2018; 62: 2–10.
2 Agarwal A, Baskaran S, Parekh N, Cho CL, Henkel R, *et al*. Male infertility. *Lancet* 2021; 397: 319–33.
3 World Health Organization. WHO Laboratory Manual for the Examination and Processing of Human Semen. 6th ed. Geneva: World Health Organization; 2021.
4 Skakkebaek NE, Lindahl-Jacobsen R, Levine H, Andersson AM, Jorgensen N, *et al*. Environmental factors in declining human fertility. *Nat Rev Endocrinol* 2022; 18: 139–57.
5 Sun H, Saeedi P, Karuranga S, Pinkepank M, Ogurtsova K, *et al*. IDF diabetes Atlas: global, regional and country-level diabetes prevalence estimates for 2021 and projections for 2045. *Diabetes Res Clin Pract* 2022; 183: 109119.
6 Bener A, Al-Ansari AA, Zirie M, Al-Hamaq AO. Is male fertility associated with type 2 diabetes mellitus? *Int Urol Nephrol* 2009; 41: 777–84.
7 Maresch CC, Stute DC, Alves MG, Oliveira PF, de Kretser DM, *et al*. Diabetes-induced hyperglycemia impairs male reproductive function: a systematic review. *Hum Reprod Update* 2018; 24: 86–105.
8 Schoeller EL, Albanna G, Frolova AI, Moley KH. Insulin rescues impaired spermatogenesis via the hypothalamic-pituitary-gonadal axis in Akita diabetic mice and restores male fertility. *Diabetes* 2012; 61: 1869–78.
9 Leisegang K, Almaghrawi W, Henkel R. The effect of *Nigella sativa* oil and metformin on male seminal parameters and testosterone in Wistar rats exposed to an obesogenic diet. *Biomed Pharmacother* 2021; 133: 111085.
10 Kumar N, Jain S, Gupta A, Tiwary AK. Spermicidal activity of sulfonylureas and meglitinide analogues: role of intrasperm Ca^{2+} elevation. *J Pharm Pharmacol* 2008; 60: 323–30.
11 Fontoura P, Cardoso MC, Erthal-Martins MC, Werneck C, Sartorio C, *et al*. The effects of liraglutide on male fertility: a case report. *Reprod Biomed Online* 2014; 29: 644–6.
12 Hallow KM, Greasley PJ, Helmlinger G, Chu L, Heerspink HJ, *et al*. Evaluation of renal and cardiovascular protection mechanisms of SGLT2 inhibitors: model-based analysis of clinical data. *Am J Physiol Renal Physiol* 2018; 315: F1295–306.
13 Wei R, Cui X, Feng J, Gu L, Lang S, *et al*. Dapagliflozin promotes beta cell regeneration by inducing pancreatic endocrine cell phenotype conversion in type 2 diabetic mice. *Metabolism* 2020; 111: 154324.
14 Pandey J, Tamrakar AK. SGLT2 inhibitors for the treatment of diabetes: a patent review (2013-2018). *Expert Opin Ther Pat* 2019; 29: 369–84.
15 Wiviott SD, Raz I, Bonaca MP, Mosenzon O, Kato ET, *et al*. Dapagliflozin and cardiovascular outcomes in type 2 diabetes. *N Engl J Med* 2019; 380: 347–57.
16 Perkovic V, Jardine MJ, Neal B, Bompoint S, Heerspink HJ, *et al*. Canagliflozin and renal outcomes in type 2 diabetes and nephropathy. *N Engl J Med* 2019; 380: 2295–306.
17 Heerspink HJ, Stefansson BV, Correa-Rotter R, Chertow GM, Greene T, *et al*. Dapagliflozin in patients with chronic kidney disease. *N Engl J Med* 2020; 383: 1436–46.
18 Raufman JP, Singh L, Eng J. Exendin-3, a novel peptide from *Heloderma horridum* venom, interacts with vasoactive intestinal peptide receptors and a newly described receptor on dispersed acini from guinea pig pancreas. Description of exendin-3(9-39) amide, a specific exendin receptor antagonist. *J Biol Chem* 1991; 266: 2897–902.
19 Vasu S, Moffett RC, Thorens B, Flatt PR. Role of endogenous GLP-1 and GIP in beta cell compensatory responses to insulin resistance and cellular stress. *PLoS One* 2014; 9: e101005.
20 Yang Y, Zhang Z, Zhang H, Hong K, Tang W, *et al*. Effects of maternal acrolein exposure during pregnancy on testicular testosterone production in fetal rats. *Mol Med Rep* 2017; 16: 491–8.
21 Jin ZR, Fang D, Liu BH, Cai J, Tang WH, *et al*. Roles of CatSper channels in the pathogenesis of asthenozoospermia and the therapeutic effects of acupuncture-like treatment on asthenozoospermia. *Theranostics* 2021; 11: 2822–44.
22 Hu X, Sui X, Li L, Huang X, Rong R, *et al*. Protocadherin 17 acts as a tumour

suppressor inducing tumour cell apoptosis and autophagy, and is frequently methylated in gastric and colorectal cancers. *J Pathol* 2013; 229: 62–73.
23 Tian Z, Yang K, Yao T, Li X, Ma Y, *et al*. Catalytically selective chemotherapy from tumor-metabolic generated lactic acid. *Small* 2019; 15: e1903746.
24 Zhu X, Li D, Du Y, He W, Lu Y. DNA hypermethylation-mediated downregulation of antioxidant genes contributes to the early onset of cataracts in highly myopic eyes. *Redox Biol* 2018; 19: 179–89.
25 Yan Y, Jiang W, Tan Y, Zou S, Zhang H, *et al*. hucMSC exosome-derived GPX1 is required for the recovery of hepatic oxidant injury. *Mol Ther* 2017; 25: 465–79.
26 Meng J, Lv Z, Qiao X, Li X, Li Y, *et al*. The decay of Redox-stress response capacity is a substantive characteristic of aging: revising the redox theory of aging. *Redox Biol* 2017; 11: 365–74.
27 Schirra J, Sturm K, Leicht P, Arnold R, Goke B, *et al*. Exendin(9-39)amide is an antagonist of glucagon-like peptide-1(7-36)amide in humans. *J Clin Invest* 1998; 101: 1421–30.
28 Dibble CC, Cantley LC. Regulation of mTORC1 by PI3K signaling. *Trends Cell Biol* 2015; 25: 545–55.
29 Zheng J, Xie Y, Ren L, Qi L, Wu L, *et al*. GLP-1 improves the supportive ability of astrocytes to neurons by promoting aerobic glycolysis in Alzheimer's disease. *Mol Metab* 2021; 47: 101180.
30 Marzook A, Tomas A, Jones B. The interplay of glucagon-like peptide-1 receptor Trafficking and signalling in pancreatic beta cells. *Front Endocrinol (Lausanne)* 2021; 12: 678055.
31 Mallidis C, Agbaje IM, Rogers DA, Glenn JV, Pringle R, *et al*. Advanced glycation end products accumulate in the reproductive tract of men with diabetes. *Int J Androl* 2009; 32: 295–305.
32 Mallidis C, Agbaje I, Rogers D, Glenn J, McCullough S, *et al*. Distribution of the receptor for advanced glycation end products in the human male reproductive tract: prevalence in men with diabetes mellitus. *Hum Reprod* 2007; 22: 2169–77.
33 Tian Y, Song W, Xu D, Chen X, Li X, *et al*. Autophagy induced by ROS aggravates testis oxidative damage in diabetes via breaking the feedforward loop linking p62 and Nrf2. *Oxid Med Cell Longev* 2020; 2020: 7156579.
34 Singh S, Malini T, Rengarajan S, Balasubramanian K. Impact of experimental diabetes and insulin replacement on epididymal secretory products and sperm maturation in albino rats. *J Cell Biochem* 2009; 108: 1094–101.
35 Attia SM, Helal GK, Alhaider AA. Assessment of genomic instability in normal and diabetic rats treated with metformin. *Chem Biol Interact* 2009; 180: 296–304.
36 Soliman GA, Abdel-Rahman RF, Ogaly HA, Althurwi HN, Abd-Elsalam RM, *et al*. *Momordica charantia* extract protects against diabetes-related spermatogenic dysfunction in male rats: molecular and biochemical study. *Molecules* 2020; 25: 5255.
37 Brown E, Heerspink HJ, Cuthbertson DJ, Wilding JP. SGLT2 inhibitors and GLP-1 receptor agonists: established and emerging indications. *Lancet* 2021; 398: 262–76.
38 Tavares RS, Escada-Rebelo S, Silva AF, Sousa MI, Ramalho-Santos J, *et al*. Antidiabetic therapies and male reproductive function: where do we stand? *Reproduction* 2018; 155: R13–37.
39 Hu Y, Xu Q, Li H, Meng Z, Hao M, *et al*. Dapagliflozin reduces apoptosis of diabetic retina and human retinal microvascular endothelial cells through ERK1/2/cPLA2/AA/ROS pathway independent of hypoglycemic. *Front Pharmacol* 2022; 13: 827896.
40 Ni L, Yuan C, Chen G, Zhang C, Wu X. SGLT2i: beyond the glucose-lowering effect. *Cardiovasc Diabetol* 2020; 19: 98.
41 Ferrannini E, Muscelli E, Frascerra S, Baldi S, Mari A, *et al*. Metabolic response to sodium-glucose cotransporter 2 inhibition in type 2 diabetic patients. *J Clin Invest* 2014; 124: 499–508.
42 Timper K, Dalmas E, Dror E, Rutti S, Thienel C, *et al*. Glucose-dependent insulinotropic peptide stimulates glucagon-like peptide 1 production by pancreatic islets via interleukin 6, produced by alpha cells. *Gastroenterology* 2016; 151: 165–79.
43 Millar P, Pathak N, Parthsarathy V, Bjourson AJ, O'Kane M, *et al*. Metabolic and neuroprotective effects of dapagliflozin and liraglutide in diabetic mice. *J Endocrinol* 2017; 234: 255–67.
44 Gasbjerg LS, Bari EJ, Christensen M, Knop FK. Exendin(9-39)NH_2: recommendations for clinical use based on a systematic literature review. *Diabetes Obes Metab* 2021; 23: 2419–36.
45 Rago V, De Rose D, Santoro M, Panza S, Malivindi R, *et al*. Human sperm express the receptor for glucagon-like peptide-1 (GLP-1), which affects sperm function and metabolism. *Endocrinology* 2020; 161: bqaa031.
46 Zhang E, Xu F, Liang H, Yan J, Xu H, *et al*. GLP-1 receptor agonist exenatide attenuates the detrimental effects of obesity on inflammatory profile in testis and sperm quality in mice. *Am J Reprod Immunol* 2015; 74: 457–66.
47 Martins AD, Monteiro MP, Silva BM, Barros A, Sousa M, *et al*. Metabolic dynamics of human Sertoli cells are differentially modulated by physiological and pharmacological concentrations of GLP-1. *Toxicol Appl Pharmacol* 2019; 362: 1–8.
48 Zhao X, Liu G, Shen H, Gao B, Li X, *et al*. Liraglutide inhibits autophagy and apoptosis induced by high glucose through GLP-1R in renal tubular epithelial cells. *Int J Mol Med* 2015; 35: 684–92.
49 Que Q, Guo X, Zhan L, Chen S, Zhang Z, *et al*. The GLP-1 agonist, liraglutide, ameliorates inflammation through the activation of the PKA/CREB pathway in a rat model of knee osteoarthritis. *J Inflamm (Lond)* 2019; 16: 13.

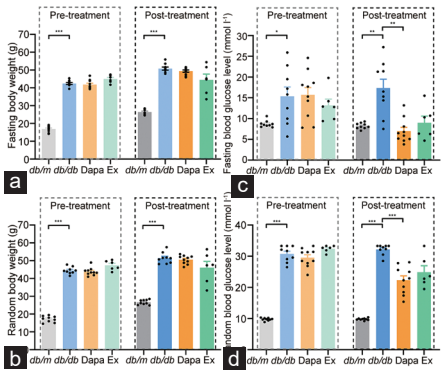

Supplementary Figure 1: Body weights and blood glucose levels of *db/m* mice and *db/db* mice treated with dapagliflozin (Dapa) and dapagliflozin + exendin (9–39) (Ex). (**a**) Fasting body weight. (**b**) Random body weight. (**c**) Fasting blood glucose levels. (**d**) Random blood glucose level. $n = 9$, 9, 10, and 6 mice in the *db/m*, *db/db*, Dapa, and Ex groups, respectively. All data are presented as the mean ± standard error of mean. $^{*}P < 0.05$, $^{**}P < 0.01$, $^{***}P < 0.001$.

Supplementary Table 1: Normality test table

Figure	*Normality test value*
Figure 1i	$t_{(39)}$=18.16 and $F_{(2, 54)}$=137.0
Figure 2a	$t_{(13)}$=8.306 and $F_{(2, 18)}$=7.011
Figure 2b	$t_{(13)}$=6.132 and $F_{(2, 18)}$=2.458
Figure 2c	$t_{(13)}$=10.15 and $F_{(2, 18)}$=8.977
Figure 2d	$t_{(13)}$=5.509 and $F_{(2, 18)}$=0.8491
Figure 2e	$t_{(13)}$=7.516 and $F_{(2, 18)}$=1.373
Figure 2f	$t_{(13)}$=7.415 and $F_{(2, 18)}$=1.764
Figure 2g	$t_{(13)}$=2.456 and $F_{(2, 18)}$=0.2287
Figure 2h	$t_{(13)}$=1.964 and $F_{(2, 18)}$=0.6304
Figure 2i	$t_{(13)}$=5.935 and $F_{(2, 18)}$=3.774
Figure 3e	$t_{(10)}$=4.557 and $F_{(2, 15)}$=11.95
Figure 3f	$t_{(15)}$=9.357 and $F_{(2, 24)}$=10.82
Figure 4b	$t_{(8)}$=12.28 and $F_{(2, 12)}$=11.77
Figure 4c	$t_{(8)}$=1.519 and $F_{(2, 12)}$=0.1930
Figure 4e	$t_{(6)}$=3.514 and $F_{(2, 9)}$=8.794
Figure 4f	$t_{(6)}$=0.5889 and $F_{(2, 9)}$=9.594
Figure 4g	$t_{(6)}$=2.735 and $F_{(2, 9)}$=2.688
Figure 4h	$t_{(6)}$=2.776 and $F_{(2, 9)}$=2.701
Figure 5a	$t_{(8)}$=3.138 and $F_{(2, 13)}$=3.525
Figure 5b	$t_{(10)}$=2.245 and $F_{(2, 15)}$=5.021
Figure 5c	$t_{(8)}$=2.753 and $F_{(2, 12)}$=3.932
Figure 5d	$t_{(8)}$=0.4946 and $F_{(2, 12)}$=0.4815
Figure 5e	$t_{(8)}$=0.8976 and $F_{(2, 13)}$=0.3305
Figure 5f	$t_{(6)}$=2.999 and $F_{(2, 9)}$=5.436
Figure 6a	$t_{(14)}$=5.226 and $F_{(2, 23)}$=21.45
Figure 6b	$t_{(6)}$=4.955 and $F_{(2, 9)}$=21.66
Figure 6c	$t_{(6)}$=2.653 and $F_{(2, 9)}$=15.13
Supplementary Figure 1a	$t_{(8)}$=32.23 and $F_{(2, 22)}$=4.172
	$t_{(8)}$=25.67 and $F_{(2, 22)}$=4.037
Supplementary Figure 1b	$t_{(8)}$=30.36 and $F_{(2, 22)}$=4.984
	$t_{(8)}$=21.71 and $F_{(2, 22)}$=2.497
Supplementary Figure 1c	$t_{(8)}$=2.889 and $F_{(2, 22)}$=0.4011
	$t_{(8)}$=4.340 and $F_{(2, 22)}$=12.22
Supplementary Figure 1d	$t_{(8)}$=22.14 and $F_{(2, 22)}$=2.513
	$t_{(8)}$=41.75 and $F_{(2, 22)}$=16.32